Received: 19 August 2019 | Revised: 22 November 2019 | Accepted: 9 December 2019

DOI: 10.1002/btpr.2950

BIOTECHNOLOGY PROGRESS

RESEARCH ARTICLE

Bioseparations and Downstream Processing

Improved packing of preparative biochromatography columns by mechanical vibration

Andrés Martinez | Konstantin Knaub | Marc Monter | Dariusch Hekmat | Dirk Weuster-Botz

Technical University of Munich, Institute of Biochemical Engineering, Garching, Germany

Correspondence
Dariusch Hekmat, Technical University of Munich, Institute of Biochemical Engineering, Garching, Germany.
Email: hekmat@lrz.tum.de

Funding information
German Federation of Industrial Research Associations, Grant/Award Number: IGF 18146 N

Peer Review
The peer review history for this article is available at https://publons.com/publon/10.1002/btpr.2950.

Abstract

The bioprocessing industry relies on packed-bed column chromatography as its primary separation process to attain the required high product purities and fulfill the strict requirements from regulatory bodies. Conventional column packing methods rely on flow packing and/or mechanical compression. In this work, the application of ultrasound and mechanical vibration during packing was studied with respect to packing density and homogeneity. We investigated two widely used biochromatography media, incompressible ceramic hydroxyapatite, and compressible polymethacrylate-based particles, packed in a laboratory-scale column with an inner diameter of 50 mm. It was shown that ultrasonic irradiation led to reduced particle segregation during sedimentation of a homogenized slurry of polymethacrylate particles. However, the application of ultrasound did not lead to an improved microstructure of already packed columns due to the low volumetric energy input (~152 W/L) caused by high acoustic reflection losses. In contrast, the application of pneumatic mechanical vibration led to considerable improvements. Flow-decoupled axial linear vibration was most suitable at a volumetric force output of ~1,190 N/L. In the case of the ceramic hydroxyapatite particles, a 13% further decrease of the packing height was achieved and the reduced height equivalent to a theoretical plate (rHETP) was decreased by 44%. For the polymethacrylate particles, a 18% further packing consolidation was achieved and the rHETP was reduced by 25%. Hence, it was shown that applying mechanical vibration resulted in more efficiently packed columns. The application of vibration furthermore is potentially suitable for in situ elimination of flow channels near the column wall.

KEYWORDS

bed compaction, column packing method, mechanical vibration, preparative biochromatography, ultrasound-assisted sedimentation

1 | INTRODUCTION

Packed-bed column liquid chromatography constitutes the main separation step for the purification of products in the bioprocessing industry.[1] Its basic principle relies on the flow of a mobile phase containing product and impurities through a packed bed composed of porous particles (the stationary phase). The interaction between the solute components and chromatographic media results in a selective separation of the target product from the impurities. Such interactions can be based on size exclusion, ion exchange, hydrophobic interaction,

affinity, or mixed mode, among others.[1] While alternative approaches to packed beds such as monolith-based columns have gained a level of acceptance in the last decades, packed-bed chromatography still represents the main method.[2]

For applications in biochromatography, compressible, spherical, porous particles based on cross-linked organic polymers such as agarose or polymethacrylate are frequently employed. Additionally, rigid, near-spherical, sintered ceramic hydroxyapatite particles,[3,4] and irregularly shaped, porous glass particles[5] are used. Regardless of particle type, an efficient column requires a porous bed packing with a homogeneous structure to avoid uneven mobile phase distribution and trans-column dispersion, which result in solute band broadening.[6,7] Furthermore, for an efficient process, the packed column should also be stable and not deteriorate over time, evident as particle rearrangement or additional consolidation during operation.[8,9] Unwanted consolidation and solute band broadening arise from the presence of void spaces formed during packing. Other packing defects can take place during operation, such as cracks in the bed, particle detachment from the column wall leading to flow channeling and formation of irregular aggregates.[10-12]

The degree of packing defects in a bed can be assessed through the packing density, which is used as a criterion to evaluate column packing protocols.[13] A bed with a high porosity usually denotes a large proportion of void spaces in its structure and often implies a low packing quality. However, it has been observed that bed homogeneity plays a larger role with regard to column efficiency than low overall bed porosity. A heterogeneous void distribution causes higher levels of hydrodynamic dispersion, which negatively affects column quality.[13] Thus, a column with a larger void volume fraction, which is more homogeneously distributed, can outperform a packing with fewer voids, which are more heterogeneously located. The higher importance of packing homogeneity compared to global bed porosity has been studied in 3D computer simulations[10] and verified experimentally.[14]

Bed porosity and homogeneity are determined by the packing method used, which mainly rely on the use of hydrodynamic flow to force a particle slurry to form a packed bed.[15] During packing of compressible resins, this is often complemented by the application of a mechanical axial force on the formed bed to achieve an additional level of axial compression.[16] The correlation between packing procedure, bed homogeneity, and solute band dispersion has been the subject of many studies,[17] and involves complex interactions of packing pressure, flow ramps, slurry concentration, and the applied bed densification steps.[18] Packing procedures are often kept a secret and are described as an art rather than a science in the open literature.[7,10,19]

Advances in particle measurement techniques and simulation capacity have allowed recent studies to focus on the examination of beds at the scale of individual particles and how such structures are affected by different packing methods. The 3D reconstruction of real packings enables the geometric analysis of their structure[20,21] or their use in posterior computer simulations.[22] Additionally, granular simulations of in silico generated packings permit the study of events difficult to access in real packings,[23] thus enabling the study of time-dependent processes such as structure evolution under operation or particle migration. Among several works following this approach,[6,13] the effect of the slurry concentration during packing on the bed structure and efficiency was studied.[18] The authors found that at higher slurry concentrations, the packing had an increased number of voids and a lessened degree of particle size segregation with the ideal concentration corresponding to a compromise between the degree of column heterogeneity and bed density.

An additional aspect of column packing is the behavior of chromatographic particles as microscopic frictional granular matter. It is well-known that such materials interact dissipatedly through inelastic collisions and a network of frictional force-chains which influence bed formation and long-term bed stability.[23,24] This was observed during the study of the influence of particle friction during the packing of two particle types with distinct and different levels of surface roughness. It was observed that smooth particles with lower friction slipped more readily during packing, resulting in a denser, albeit more inhomogeneous, microstructure. In comparison, media with rougher surfaces resisted movement under consolidation and delivered less dense and more homogeneous structures.[14]

Furthermore, the granular properties of the packed bed also determine stability during operation. It has been previously established that granular packings come to rest in a jammed state which may be far from the most stable and dense configuration.[25] In such a metastable state, the structure is stabilized through cooperative frictional structures of several particles, forming bridges or arches which enable the packing to withstand external loads and behave locally as a solid.[26] These structures are also responsible for the formation and persistence of void spaces.[27] Unless perturbed by an external force, the system remains static[24] and is unable to reach its most homogeneous structure.[15,23] To escape the meta-stable state, energy must be supplied to the system. External perturbations can unlock the packing and allow the structure to explore the phase space[24] and densify the packing as particles fill void spaces made accessible by bridge collapses.[28] This principle also applies to chromatographic beds and it has been argued to be the only means to minimize packing defects.[10]

Granular densification is a matter of interest for various industries with different applied approaches such as thermal cycling,[29] mechanical vibration,[28] ultrasound irradiation,[30,31] upward flow,[32] wall oscillation,[33] packing through viscous flow drag, mechanical pressing, and combinations thereof.[34] Mechanical vibration and ultrasonification have been extensively applied for the compaction of granular matter in several fields, for example, soil compaction in oil exploration,[35] pharmaceutical tablet pressing,[36,37] and compaction of bodies in the metallurgic industry,[38,39] among others.

The application of ultrasound for the packing of chromatographic media has been studied in thin capillaries from micrometer range[40,41] up to 4.6 mm in diameter,[42] and microchips at the micrometer scale.[43] In most cases, the capillaries were submerged in an ultrasonic bath. While some studies carried out a simultaneous ultrasound irradiation of the capillaries with flow packing,[7,41] others decoupled both processes.[40] Though some authors reported the packing of more efficient and stable columns measured by improved values of the height

equivalent to a theoretical plate (HETP), it was also found that ultrasonic vibrations can cause the bed to become more heterogeneous.[42]

The use of mechanical vibration to achieve further compaction in chromatographic beds has also been studied previously. However, this has only been performed using rigid, nonspherical, irregularly shaped, porous glass-based media.[15,44] Furthermore, these studies were limited to the application of a rotational type of pneumatic vibrators.

In this work, we investigate the use of ultrasound during sedimentation of compressible polymethacrylate chromatographic particles in a column with an inner diameter of 50 mm. An ultrasonic transducer was integrated into the bottom flange of the column in direct contact with the column internal space. Furthermore, the application of mechanical vibration was studied during packing of incompressible ceramic hydroxyapatite particles and compressible polymethacrylate particles in this 50 mm column. The influence of different parameters such as vibrator type, direction of vibration, and duration of vibration was studied. The implemented packing method was quantified in terms of the expected improved column performance and compared with conventional packing methods. Finally, the use of mechanical vibration for the in situ correction of packing defects in the 50 mm column was explored.

2 | EXPERIMENTAL METHODS

2.1 | Chemicals and materials

Acetone and sodium di-hydrogen phosphate monohydrate were purchased from Carl Roth GmbH & Co. (Karlsruhe, Germany). Sodium hydroxide was acquired from NeoFroxx GmbH (Einhausen, Germany). CHT ceramic hydroxyapatite particles and Toyopearl SP-650M were generously provided by Bio-Rad Laboratories GmbH (Munich, Germany) and Tosoh Bioscience GmbH (Stuttgart, Germany), respectively. CHT ceramic hydroxyapatite is an incompressible mixed-mode chromatography media made of a near-spherical, macroporous form of hydroxyapatite. In this study, CHT particles type I with a mean particle diameter of 40 μm were used. For CHT particles, a working buffer of 500 mM NaOH and 50 mM NaH_2PO_4 was used. Toyopearl SP-650M is a compressible anion exchange resin with a porous polymethacrylate base matrix with a mean particle diameter of 65 μm. For Toyopearl particles, a solution of 10 mM NaOH was employed.

2.2 | Flow equipment

Flow for the packing procedures was provided by a computer-controlled precision gear pump (micropump GB-P25.JVS.A, Idex Health & Science, Oak Harbor, WA). Flow rate was measured using an inductive flow meter (Promag 50 H, Endress+Hauser, Weil am Rhein, Germany). Column pressure drop was obtained using a digital pressure gauge (692.30111151, Huba Control, Walddorfhäslach, Germany). The pump was controlled using a PID control system implemented in LabView (National Instruments, Austin, Texas) so that a desired flow rate or pressure drop profile could be achieved. All elements of the control system were connected to the computer through a USB-6008 data acquisition interface from National Instruments (Munich, Germany).

For the injection of samples and generation of chromatograms, a pulse-free gear pump type Tuthill DGS.19PPPT2NNBG45 (Wagner Mess-und Regeltechnik GmbH, Offenbach, Germany) was employed. Flow was controlled and measured by a Coriolis-type Bronkhorst High-Tech M13-RAD-22-K-S. The pressure was controlled by a digital pressure controller type Bronkhorst High-Tech P-502C-21KR-RAD-33-V (Wagner Mess-und Regeltechnik GmbH, Offenbach, Germany).

Chromatograms were generated by injecting an aqueous solution of 2% vol/vol acetone in the respective working solution using an injection loop with a constant volume of ~2% of column volume. Chromatograms were made employing a UV-spectrophotometer (SPD-20A, Shimadzu Deutschland GmbH, Neufahrn bei Freising, Germany) fitted with a preparative flow cell (228-23406-91, Shimadzu) with an optical path of 0.5 mm and a total volume of 6.5 μl. Analogue absorption data from the photometer was gathered employing a 16-bit analogue-to-digital converter ADS1115 (Adafruit Industries, NY) connected to a Raspberry Pi (Raspberry Pi Foundation, Cambridge, United Kingdom). Data were logged employing a custom script written in Python 3.0. Collected data were analyzed with MATLAB 2017b (Mathworks, Natick, MA) for the calculation of HETP.

The sedimenting slurry height and the compression behavior of the chromatographic beds were tracked by photographs taken with a Canon EOS 80D equipped with a Canon EF 100/2.8 L IS Macro USM objective. The images were calibrated using markings on the column of known length and analyzed using MATLAB 2017b. All experiments were carried out at 25°C employing a KISS K25 bath thermostat manufactured by Huber Kältemaschinenbau AG (Offenburg, Germany) in which all solutions were kept.

Ultrasonic waves were generated with an ultrasonic transducer type E/805/T/M/S powered by a signal generator type MFG (Meinhard Ultraschalltechnik GmbH, Leipzig, Germany). The transducer had a stainless steel active face with a diameter of 15 mm with resonant frequencies were 835, 1,350, and 2,500 kHz. The signal generator was set up to deliver a maximal power of 125 W. The frequency with the highest measured acoustic intensity was 835 kHz which was used for all experiments.

Pneumatic vibrators of type K-8 and FP-12-S were acquired from Aldak Vibrationstechnik (Troisdorf, Germany). Pressurized air was filtered with a 50 μm metal-sinter air filter and lubricated using a mist oiler as indicated by the manufacturer. Air pressure was controlled with a precision valve and a gauge. K-8 ball-type vibrators are based on the rotation of a hardened steel ball along a circular steel guide, which creates the vibration due to the centrifugal force of the moving ball. Rotation-based vibrators deliver the force in the direction of rotation, thus the vibration does not propagate strictly perpendicularly from the vibrator[45] and possesses a tangential component in relation to the vibrator's surface normal. In contrast, piston-type vibrators such as the FP-12-S generate linear vibrations through the oscillation of a cylindrical piston inside the vibrator housing. The piston is

accelerated, decelerated, and reversed by the pressurized air, resulting in a sinusoidal vibration profile, which propagates perpendicularly from the vibrator's surface.

2.3 | Columns

The columns were made from a poly(methyl methylacrylate) (PMMA) cylinder with an inner and outer diameter of 50 and 60 mm, respectively, with a static and a movable flow distributor which could be placed either at the top or the bottom of the column. Flow distributors were machined out of stainless steel and fitted with a stainless steel frit with a mean pore size of 8 μm (Tridelta Siperm GmbH, Dortmund, Germany) to retain the particles. The movable distributor was attached to a trapezoidal screw allowing the column height to be changed, and the distributor to be driven without rotating.

2.4 | Internal ultrasound transducer

A custom flow distributor was built to house the ultrasonic transducer and enable a direct contact with the particle packing to avoid acoustic losses caused by material between the ultrasound source and the column internal space. The transducer was positioned in the central axis of the distributor (Figure 1) enabling the passage of fluid through a ring-shaped region with three radially distributed outlet ports which were covered with a stainless steel frits. An O-ring was placed between the transducer and flow distributor to seal the joint. The distributor housing the transducer was placed at the bottom of the column.

2.5 | Pneumatic vibration

The vibrators were attached to the column in two possible configurations, lateral or axial. In the lateral case, the vibrators were fixed near the bottom of the column outer wall using a PMMA clamp (Figure 2).

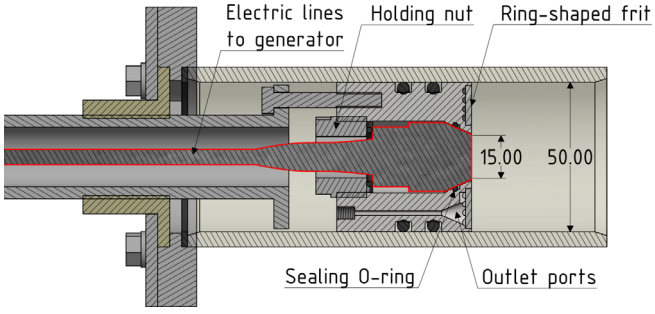

FIGURE 1 Schematic sketch of the flow distributor of the column with an inner diameter of D = 50 mm incorporating the ultrasound transducer (red outline). The ultrasound transducer is located in the central column axis in direct contact with the column interior. Measurements in millimeters

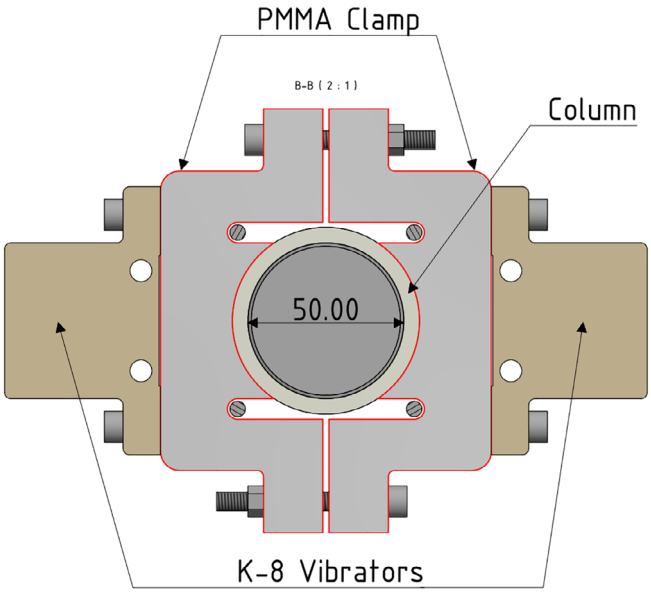

FIGURE 2 Schematic sketch in top–down view of the two K-8 rotational vibrators attached laterally near the bottom of the 50 mm column employing PMMA clamps (red outline). Measurements in millimeters

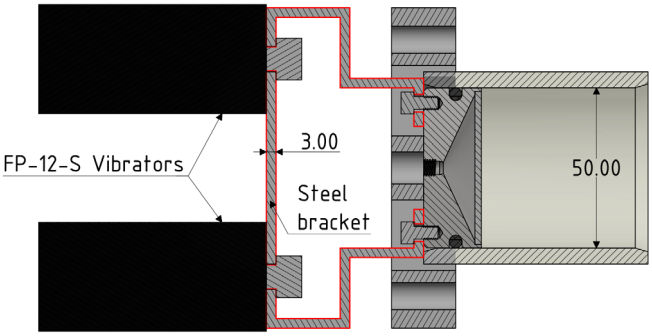

FIGURE 3 Schematic sketch of two FP-12-S linear vibrators attached to the bottom flow distributor of the 50 mm column by a steel bracket (red outline). Alternatively, a single K-8 rotational vibrator was attached to the steel bracket (not shown). Measurements in millimeters

In the axial case, the vibrators were attached to a V2A steel bracket directly connected to the flow distributor through two apertures in the bottom flange of the column (Figure 3).

2.6 | Experimental procedures

2.6.1 | Ultrasound experiments

The behavior of a suspension of chromatographic particles was studied during sedimentation in an ultrasonic field. Toyopearl SP-650M were chosen due to their slower gravity settling velocity of ~20 cm/h in comparison to CHT particles at 180 cm/h which would settle too

quickly for an accurate measurement.[46,47] Enough particles to achieve a packed bed height H = 50 mm (height to diameter ratio [H/D] of 1) were introduced in the column containing the flow distributor with the ultrasound transducer. The distance between flow distributors was set to 100 mm to achieve a slurry concentration of 50% vol/vol after resuspending the packing, which was achieved by applying flow in the upward direction. Complete resuspension of the particles was obtained by slightly tapping the outer column wall manually. Upward flow was stopped once the slurry reached a distance of around two millimeters below the top flow distributor. Once a homogeneous suspension was achieved, the particles were allowed to settle either by gravity only or in the presence of an ultrasonic field. For the generation of the ultrasonic field, a continuous signal of 125 W peak power with a frequency of 835 kHz was supplied to the transducer. The active area of the ultrasound transducer was made of chemically inert stainless steel. This enabled a direct contact with the mobile phase, but caused high acoustic reflection at the steel-water interface due to the difference in acoustic impedances, Z = 1.5 MRayl and Z = 46.9 MRayl for water and steel, respectively.[48] Wave reflection is given by the formula $R = \left|\frac{Z_0 - Z_1}{Z_0 + Z_1}\right|^2$, where Z_0 and Z_1 are the impedances of each material at the interface.[49] For a steel-water system 88% of the ultrasonic wave is reflected. A transducer active face with a lower acoustic impedance can be achieved by employing doped polymeric layers acoustically matched to water,[50] such as silicones or epoxies. Although these possess a higher acoustic efficiency, they lack the chemical resistance of stainless steel. Thus, effective acoustic work in the column was ~76 W/L, based on the particle slurry volume, or 152 W/L based on consolidated bed volume. The consolidation of the particle bed was determined by measuring the decreasing packing height optically with high precision using a camera type Canon EOS 80D equipped with an EF 100 mm f/2.8 L Macro IS USM objective.

2.6.2 | Preliminary pneumatic vibration experiments

The compression-relaxation dynamics at the single particle level play a role during the packing of chromatographic beds composed of compressible media.[51] Particle compressibility is a function of bead internal porosity and rigidity of the matrix material. Resins based on cross-linked organic polymers, such as Toyopearl SP-650M, which have an internal porosity of 63%,[52] readily deform under stress and introduce additional compression effects. Thus for the preliminary studies, CHT particles were chosen due to their incompressibility to exclude any possible compression-relaxation effects at the bead level caused by particle viscoelasticity.[12] The goal of the preliminary experiments was to identify suitable vibration parameters. Bed height was set to a H/D of 2. The initial step for the following experiments was the resuspension of the particle slurry inside the column. This was done by employing an upward flow and light mechanical agitation by slightly tapping the outer column wall manually. For all experiments, the compaction of the bed was defined as $\lambda\,[\%] = \frac{H_0 - H}{H_0} * 100$, where H_0 is the initial height of the packing and H is the packing height after applying vibration.

2.6.3 | Coupled and decoupled vibration

Prior to studying the different vibrator types and configurations, the influence of flow through the packing as a possible reinforcement factor of granular force-chains was studied. The vibrators were attached laterally to the column and two types of vibration experiments were carried out. During coupled vibration experiments, the vibrators were turned on simultaneously as fluid was pumped through the bed. In decoupled experiments, the vibrators were turned on only when there was no flow through the packing. In decoupled experiments, the flow was slowly ramped up during 30 s and held for 2 min at a preset target flow rate before ramping down during 30 s. The flow rates were computer-controlled to ensure high precision and repeatability. The packed bed was completely consolidated after ~5 s after the target flow rate was reached. The vibrators were turned on once no fluid was observed to be flowing through the packing. In coupled vibration experiments, the same ramping times as above were kept while the consolidation flow was maintained at all times. The vibrators were turned on once the initial ramp reached the target flow rate and were stopped as the ramping down started. Both coupled and decoupled experiments were carried out at superficial velocities of the mobile phase of 300 and 600 cm/h.

2.6.4 | Lateral vibration

Vibrators were placed near the column bottom so that vibrations entered the packing laterally from the column wall. Two K-8 ball vibrators were clamped on opposite sides with mirrored configurations. After resuspension, the slurry was consolidated at 300 cm/h with the same ramp times as in the decoupled experiments. Once the flow stopped, the vibrators were turned on for up to 60 min with an air pressure of 2 bar. Industrial pneumatic vibrators were chosen and dimensioned according to their output force rating (instead of a power rating which is available only for electromagnetic vibrators).[45] According to the manufacturer, the K-8 vibrator had a frequency of 417 Hz and a centrifugal force of 130 N when operating at 2 bar. Thus, ~1,326 N/L were applied to the consolidated bed with a H/D of 2 during lateral vibration.

2.6.5 | Axial vibration

Two vibrator types were explored in the axial study. Either a single K-8 ball vibrator or two FP-12-S linear vibrators were attached to the bottom flow distributor with a steel bracket. For the K-8 vibrator, a volumetric force of 683 N/L was employed. After resuspension, the slurry was consolidated at 300 cm/h with the same ramp times as in the decoupled experiments. Once the flow stopped, the vibrators

were turned on for up to 60 min with an air pressure of 2 bar. According to the manufacturer, a FP-12-S vibrator had a frequency of 103 Hz and a force of 34 N when operating at 2 bar.[53] This corresponded to a volumetric force of 347 N/L acting on the consolidated bed with a H/D of 2.

2.7 | Pneumatic vibration packing and column quality testing

Packing procedures for CHT and Toyopearl particles were derived from the respective manufacturer's notes and guidelines.[46,47] For both particle types, the starting point was a homogeneous particle suspension obtained again through upward flow and mechanical agitation by slightly tapping the outer column wall manually. A H/D of 0.5 was chosen to replicate common conditions found in large-scale preparative columns.[15]

2.7.1 | CHT ceramic hydroxyapatite vibration packing

The standard CHT-packing procedure was a single flow-packing step with no mechanical compression due to the rigid nature of the sintered particles.[47] The column fill height was set to obtain a slurry concentration of 33% vol/vol following the manufacturer's packing advice.[47] The packing procedure was started by linearly increasing the downward flow during 30 s until a target flow rate of 300 cm/h was reached which was then held for 2 min.[3] This was followed by a linear decrease of the flow rate for 30 s until flow was completely stopped (applying more than one packing step or longer flow times did not appreciably further compact the bed). The upper flow distributor was then moved downwards with the inlet valve opened and the outlet valve closed to avoid disruption of the bed. Since mechanical compression was to be avoided, a 1 mm gap between flow distributor and the top of the bed was left to prevent particle damage.[47] During vibration experiments, the vibrators were turned on for 20 min with an air pressure of 1.5 bar after the flow was stopped and before the upper flow distributor was moved downwards. The chosen air pressure was lower compared to the preliminary experiments to compensate for the shorter bed, achieving a volumetric force of ~1,190 N/L acting on the consolidated bed with a H/D of 0.5. Air pressures lower than 1.5 bar resulted in an irregular operation of the vibrators and were thus not explored.

2.7.2 | Toyopearl SP-650M vibration packing

The column fill height was set to obtain a slurry concentration of 50% vol/vol after particle resuspension following the manufacturer's packing advice.[46] The basis of Toyopearl SP-650M standard packing are multiple iterations of flow packing steps. Each flow packing step consisted of a ramp-up of 60 s until a superficial velocity of 800 cm/h was reached and held for 5 min, followed by a 60 s ramp-down until the flow was stopped which was held for 5 min. This flow packing step was then repeated twice (carrying out more than three flow packing steps did not further compact the bed). Finally, the flow distributor was driven 2 mm into the bed with the inlet valve open and outlet valve closed. This was equivalent to an axial compression of 7%. During vibration experiments, the vibrators were turned on only once, after the first flow packing step for 25 min with an air pressure of 1.5 bar. Vibrating for more than 25 min resulted in a negligible additional compaction.

2.7.3 | Column quality testing

Once packed, the beds were equilibrated at a constant flow of 100 cm/h until ultraviolet absorbance at 265 nm of the effluent liquid became stable. Elution chromatograms of the aqueous solution of 2% acetone were measured in triplicate and the resulting peaks were employed to calculate the quality of the packing. HETP was defined as:

$$HETP = \frac{L}{5.54} * \left(\frac{W_{50\%}}{t_r}\right)^2, \quad (1)$$

where L is the bed height, t_r the retention time of the acetone peak, and $W_{50\%}$ the peak width at half peak height. HETP was divided by the respective mean particle diameter to obtain the reduced HETP (rHETP). Asymmetry was defined as:

$$As = \frac{b}{a}, \quad (2)$$

where a is the peak width (left half) at 10% of peak height and b the peak width (right half) at 10% peak height.

3 | RESULTS AND DISCUSSION

3.1 | Sedimentation of a chromatographic slurry in an ultrasonic field

The difference in settling behavior of polymethacrylate particles between ultrasound-assisted sedimentation and the standard case without ultrasound can be seen in Figure 4, in which the change in time of the slurry height is shown for both cases.

The time course during ultrasound-assisted settling was sigmoidal. Sedimentation was slow in the beginning but increased with time. A relatively high sedimentation rate was observed before the final packing height was reached. In contrast to this, the time course of the gravity settling was linear at a lower sedimentation rate until the final packing height was reached. However, the obtained ultrasound-assisted packing consolidation was only ~1% higher compared to gravity settling.

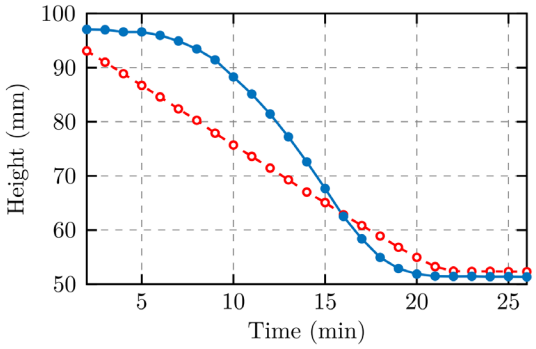

FIGURE 4 Settling progression of polymethacrylate particles in an ultrasonic field (continuous line with closed markers) and gravity-only case (dashed line with open markers)

The ultrasound-assisted settling behavior can be explained by the acoustic effects. In general, the application of an ultrasonic field in a fluid can generate two distinct phenomena: acoustic streaming and acoustic radiation forces.[54] While several types of acoustic streaming can be defined,[55] the most relevant type is Eckart streaming which arises from the attenuation of sound waves as these propagate in the medium. The front of the transducer forms a high pressure zone. As acoustic energy diminishes along its trajectory, zones of low pressure are formed. Thus, a net fluid movement from high to low pressure regions is created with an orientation perpendicular to the transducer face. Since in our case the transducer was located at the bottom of the column with an upward propagation direction, acoustic streaming acted against gravity and resulted in a delayed initial settling behavior.

Acoustic radiation forces can explain the later observed increase of the settling velocity. Travelling waves of an ultrasonic field in a fluid create pressures nodes and antinodes, which interact and can either attract or repel suspended particles depending on their properties.[56] In our system, the particles were attracted to and collected in the pressure nodes. As the particles group along the nodal planes, they form clusters with a decreased surface to volume ratio equivalent to "super-particles" with an increased settling velocity.[57] This effect explains the observed accelerated settling. As particles of different sizes agglomerate, they form a denser structure in contrast to Stokes sedimentation. In the latter case, particles settle according to their size with the larger particles at the bottom and the smaller ones at the top resulting in an unwanted particle segregation.

Once the bed had consolidated, the application of ultrasound caused no further change in the packing. Further experiments also showed no or very little effect of ultrasonic vibrations in already consolidated beds. A possible explanation is that the magnitude of the generated ultrasonic waves was not high enough to overcome the frictional resistance of the particles in the consolidated packings in order to accomplish particle rearrangement. Consequently, the application of mechanical vibration using pneumatic vibrators was explored. These not only generate larger amplitudes than ultrasonic waves but also experience lower acoustic attenuation, which is proportional to the wave frequency. While ultrasonic waves propagate at frequencies starting at 20 kHz, pneumatic vibrators commonly oscillate in the three-digit Hz range. Hence, mechanical vibration can deliver higher energy and the mechanical waves are less attenuated as they propagate.

3.2 | Pneumatic vibration experiments

3.2.1 | Vibration with coupled and decoupled flow

Vibration with simultaneous flow through the bed did not deliver any appreciable further compaction at either 300 or 600 cm/h. In comparison, vibration decoupled from flow clearly led to additional compaction, with beds packed at 300 cm/h consolidating from 100 ± 0.3 mm down to 89.9 ± 0.7 mm after 60 min of vibration (N = 3), corresponding to a compaction of 10.2%. Beds packed at 600 cm/h and subsequently vibrated showed similar compaction values. This can be explained by the effect of the fluid viscous drag on the particles in the packing. The flow exerts a net downwards force on the bed, which is transmitted to the column wall through granular arches forming a force-chain network.[23] Analogous to arches in architecture, granular arches act as support structures and sustain the weight of the material above them.[58] Fluid flow thus acts as a reinforcement of the structure and prevents the displacement of particles and compaction of the packing through vibration. All following experiments were consequently carried out in the decoupled mode.

3.2.2 | Lateral and axial vibration

It was observed that lateral vibration caused an inhomogeneous radial compaction of the bed with the outer region of the packing being further compacted than the central region. This was evident as the formation of a plateau in the center with a height of about 2 mm above the rest of the bed (Figure 5).

Furthermore, elution chromatograms displayed two distinct peaks indicating a more pronounced mobile phase flow through the inner region of the column (data not shown). Axial vibration with a rotational K-8 ball vibrator showed a macroscopically homogeneous

FIGURE 5 Plateau in the central region of the top of a CHT packing formed after 60 min of lateral vibration. The distance between horizontal markings is 10 mm (column adapter moved up for visibility of packing top)

packing with no appreciable plateau formation. However, the elution chromatogram again exhibited a double peak indicating the formation of a heterogeneous packing at the microstructural level. This was most probably caused by tangential forces generated by the rotational vibrators. Axial vibration employing two linear FP-12-S piston vibrators not only showed a macroscopically homogeneous compaction of the packing but also displayed a single peak in the elution chromatogram. Therefore, the packing experiments were consequently carried out in the decoupled mode, employing axial vibration using two linear vibrators.

3.3 | Axial vibration packing and column quality testing

3.3.1 | CHT ceramic hydroxyapatite

Once the bed was packed following the manufacturer's flow packing protocol, axial linear vibration was applied until no further compaction was observed. The change of the bed height over time caused by vibration is exemplarily shown for a single packing in Figure 6.

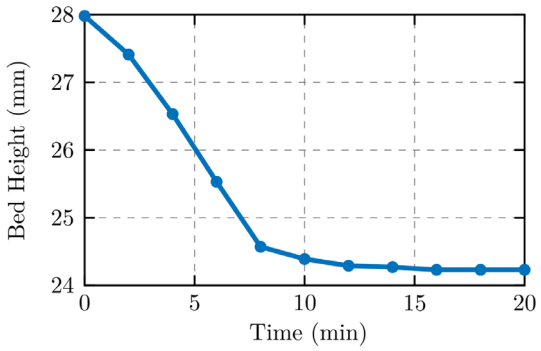

FIGURE 6 Height evolution of a flow packed CHT packing under axial linear vibration decoupled from flow. Additional bed height compaction was 3.7 mm (λ = 13%)

On average, the height of the flow packed bed before vibration was 28.3 ± 0.03 mm (N = 3) while the vibrated bed reached 24.3 ± 0.05 mm (N = 2). This meant a further compaction through vibration of 13 ± 0.2%. A rapid compaction during the first 8 min of vibration was followed by a period of significantly slower compaction. The observed time course agrees with theoretical work on vibration of granular materials describing the densification of packings as an inverse exponential process.[28] As the bed becomes denser, additional compression requires the simultaneous rearrangement of an increasingly larger number of particles, thus becoming less frequent.[59]

The homogeneity of the achieved bed was tested by tracer experiments and the calculation of asymmetry factor and rHETP. Figure 7a shows the elution chromatograms for standard and vibration-assisted CHT packings. Figure 7b shows the rHETP of standard and vibration-assisted packing. The asymmetry factor of the standard packing was 4.6 ± 0.3 while the asymmetry factor of the vibration packed columns was reduced to 3.3 ± 0.3. Furthermore, a reduction from the standard packing rHETP of 5.5 ± 0.6 down to 3.1 ± 0.26 for the vibration packing was obtained, constituting an improvement of 43.6%. The high absolute values of asymmetry and rHETP stem from the fact that the extra-column volume of the experimental set-up was large leading to band broadening.[60]

3.3.2 | Toyopearl SP-650M

Analogous as for CHT, the application of vibration during packing substantially compressed the bed and delivered a more efficient column. On average, the height of the bed after standard packing before vibration was 27.7 ± 0.5 mm (N = 3) while the vibrated bed reached 23.3 ± 0.2 mm (N = 3). This meant a further compaction through vibration of 18 ± 0.9%. The change of the bed height over time caused by vibration is exemplarily shown for a single Toyopearl SP-650M packing in Figure 8.

The higher compaction degree in comparison to CHT can be attributed to the mechanical properties of polymethacrylate particles being less dense, more compressible, and having a smoother surface

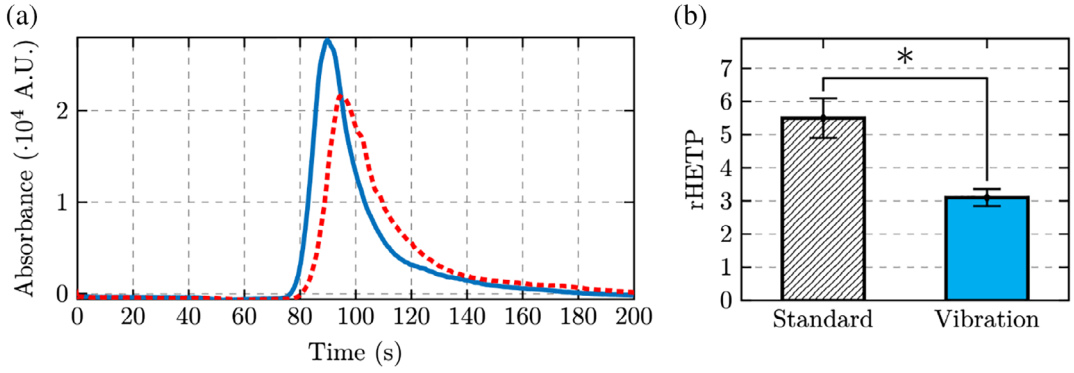

FIGURE 7 (a) Elution chromatograms for standard (dashed line) and vibration-assisted (solid line) CHT packings. (b) rHETP of standard and vibration-assisted CHT packings (*p < = .01)

compared to CHT particles resulting in less resistance to particle rearrangement due to lower friction between particles.

Figure 9a shows the elution chromatograms for standard and vibration-assisted polymethacrylate packings. Figure 9b shows the rHETP of the standard and vibration-assisted packing. The asymmetry factor of the standard packing was 4.4 ± 0.9 while the asymmetry factor of the vibration packed columns was reduced to 3.7 ± 0.5. A reduction from the standard packing rHETP of 14.3 ± 0.5 down to 10.8 ± 1.4 for the vibration packing was obtained, constituting an improvement of ~24.5%. Again, high absolute values of asymmetry and rHETP were obtained because of the large extra-column volume of the experimental set-up.

The smaller improvement of polymethacrylate column efficiency in comparison to CHT can be explained by the additional mechanical compression step after flow packing of the column. As the upper flow distributor was pressed 2 mm into the bed during the final packing step corresponding to a compaction factor λ = 7%, the void spaces of the structure were further reduced. The packing structure was thus already denser in comparison to the solely flow-packed CHT structure. As the porosity of standard-packed polymethacrylate column was smaller, there was comparatively less room for improvement through vibration.

For both media types, no increase of the turbidity of the effluent liquids from the columns was observed. Hence, it can be assumed that no particle breakage or formation of fines took place at the vibration levels applied. Additional experiments with vibrations at higher air pressures were explored. It was found that stronger vibrations caused the bottom of the packing to rise and expand somewhat randomly forming pockets of void spaces near the fluid distributor. Previous works have reported that at too high vibration amplitudes, granular bridge collapse is disorganized and as much void space is created during each cycle as is reduced in the previous one resulting in no overall densification.[59]

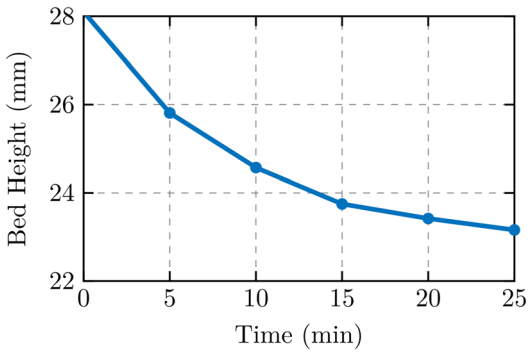

FIGURE 8 Height evolution of a flow packed polymethacrylate packing under axial linear vibration decoupled from flow. Additional bed compaction was 4.9 mm (λ = 18%)

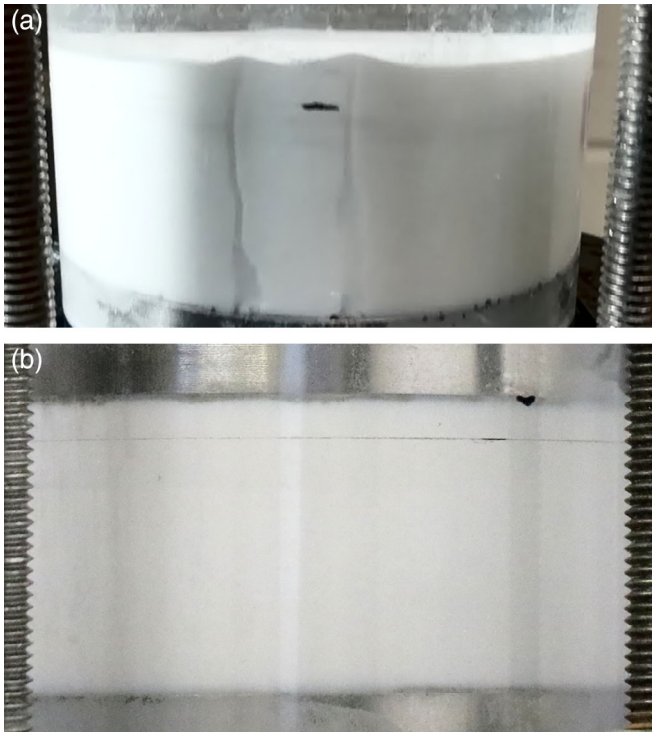

FIGURE 10 (a) Flow channeling during standard packing of a polymethacrylate column. Photo taken after flow packing before mechanical compression. (b) Polymethacrylate bed after mechanical compression, no channeling was observed

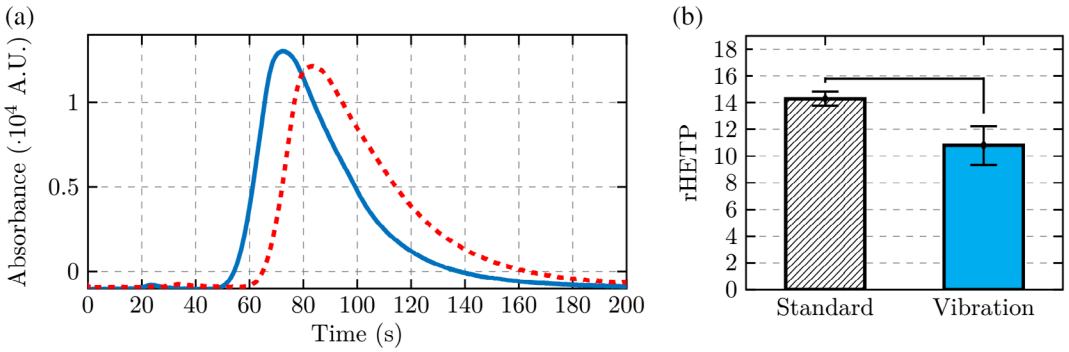

FIGURE 9 (a) Elution chromatograms for standard (dashed line) and vibration-assisted (solid line) polymethacrylate packings. (b) rHETP of standard and vibration-assisted polymethacrylate packings (p < .05)

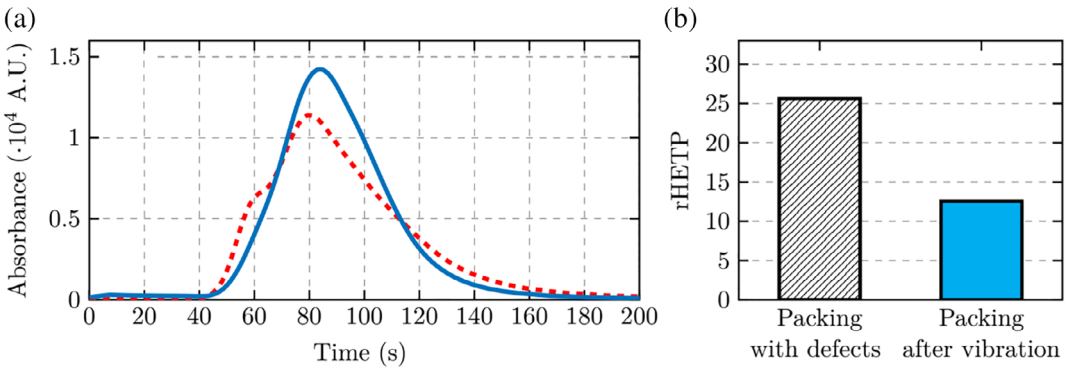

FIGURE 11 (a) Elution chromatograms of polymethacrylate packings. Dashed line: Peak fronting due to flow channeling (see Figure 10). Continuous line: After 25 min of axial linear vibration. (b) rHETP of a polymethacrylate packing with flow channels and after 25 min of axial linear vibration

Besides the improved efficiency of the vibrated columns using both types of particles, the columns are also expected to be more stable under long-term operation since the packings reach a denser, more homogeneous state.

3.4 | In situ correction of packing defects

The possibility of employing vibration for the in situ correction of bed defects in already packed columns was explored. During a standard flow packing experiment of Toyopearl SP-650M, it was observed that flow channels were formed near the wall of the column due to the presence of air bubbles during flow packing (Figure 10a).

The channels remained during the flow packing steps, after which the upper flow distributor was moved 2 mm into the bed following the standard packing protocol. At this point, the compressed bed appeared macroscopically homogeneous with no visible channeling at the wall. However, packing inhomogeneities were evident from the elution chromatogram as a fronting shoulder (dashed line in Figure 11a). Figure 11b shows the rHETP of a polymethacrylate packing with flow channels and the same packing after 25 min of axial linear vibration. The rHETP of 25.6 was approximately double that of the standard rHETP of 14.3. Asymmetry of the packing with defects was 2.22. The axial linear vibrators were turned on for 25 min after which elution chromatograms were repeated. While no macroscopic changes in the column were observed, the chromatograms showed that the efficiency was improved to a rHETP of 12.5 and an asymmetry of 1.53. The lower asymmetry values in comparison to the defect-free packing arose from the peak fronting which increased the term a in Equation (2), thus compensating for the peak tailing.

4 | CONCLUSIONS

Biochromatography columns packed by conventional methods frequently do not reach their most dense state and their packing structure is not as homogeneous as possible. The generation of an ultrasonic field inside the column can be used to delay the onset of particle sedimentation. This is achieved by acoustic streaming and acoustic radiation forces, which keep the particle slurry longer in suspension, and thus may reduce the level of particle segregation due to varying size-dependent sedimentation velocities. Vibration-assisted packing implemented through flow-decoupled axial linear vibration led to considerably denser and more homogeneous packings of two widely used biochromatography media, incompressible ceramic hydroxyapatite and compressible polymethacrylate particles. This was shown by clearly improved rHETP values. Mechanical vibration can also be applied on already packed beds to improve column packing homogeneity in situ, thus avoiding costly re-packing procedures. The developed technologies can be implemented for packing of process columns to improve biomanufacturing processes due to improved chromatographic efficiency. Furthermore, it is conceivable that an enhanced column reliability may be achieved by a diminished level of particle rearrangement and consequently reduced headspace formation during long-term operation.

Therefore, further work should focus on the scale-up of the developed vibration packing method to larger process columns. This could take place in custom-built columns enabling the attachment of several linear vibrators to the bottom side of the columns which can be dimensioned using the force-to-volume ratios used in this work as a starting point. However, commercially available industrial columns presently have fixed process pipes and manifolds on the bottom side of the columns which restrict a symmetrical mounting of multiple vibrators. This could negatively influence the achievable level of homogeneity of the vibrated beds.

ACKNOWLEDGMENTS

The authors acknowledge the kind provision of CHT ceramic hydroxyapatite® by Bio-Rad Laboratories GmbH, Munich, Germany, and Toyopearl SP-650M® by Tosoh Bioscience GmbH, Stuttgart, Germany. The research project was carried out in the framework of the industrial collective research programme (IGF no. 18146 N). It was supported by the Federal Ministry for Economic Affairs and Energy (BMWi) through the AiF (German Federation of Industrial Research Associations eV)

based on a decision taken by the German Bundestag. The additional support of Andrés Martinez by the TUM Graduate School, Technical University of Munich, Germany, is gratefully acknowledged.

CONFLICT OF INTEREST

The authors declare no financial or commercial conflict of interest.

ORCID

Dariusch Hekmat https://orcid.org/0000-0003-0263-232X

REFERENCES

1. Guiochon G, Beaver LA. Separation science is the key to successful biopharmaceuticals. *J Chromatogr A*. 2011;1218(49):8836-8858.
2. Guiochon G. Monolithic columns in high-performance liquid chromatography. *J Chromatogr A*. 2007;1168(1–2):101-168.
3. Cummings LJ, Snyder MA, Brisack K. Protein chromatography on hydroxyapatite columns. *Guide to Protein Purification*. 2nd ed. Cambdrige, Massachusetts: Academic Press; 2009:387-404.
4. Gagnon P. Monoclonal antibody purification with hydroxyapatite. *N Biotechnol*. 2009;25(5):287-293.
5. Siu SC, Chia C, Mok Y, Pattnaik P. Packing of large-scale chromatography columns with irregularly shaped glass based resins using a stop-flow method. *Biotechnol Prog*. 2014;30(6):1319-1325.
6. Bruns S, Tallarek U. Physical reconstruction of packed beds and their morphological analysis: Core–shell packings as an example. *J Chromatogr A*. 2011;1218:1849-1860.
7. Godinho JM, Reising AE, Tallarek U, Jorgenson JW. Implementation of high slurry concentration and sonication to pack high-efficiency, meter-long capillary ultra-high pressure liquid chromatography columns. *J Chromatogr A*. 2016;1462:165-169.
8. Günter J, Sofer G, Hagel L. Column packing. *Handbook of Process Chromatography: Development, Manufacturing, Validation and Economics*. Cambridge: Academic Press; 2007:321-330.
9. Guiochon G, Sarker M. Consolidation of the packing material in chromatographic columns under dynamic axial compression. I. Fundamental study. *J Chromatogr A*. 1995;704:247-268.
10. Schure MR, Maier RS. How does column packing microstructure affect column efficiency in liquid chromatography? *J Chromatogr A*. 2006;1126:58-69.
11. Reising AE, Godinho JM, Hormann K, Jorgenson JW, Tallarek U. Larger voids in mechanically stable, loose packings of 1.3 μm frictional, cohesive particles: their reconstruction, statistical analysis, and impact on separation efficiency. *J Chromatogr A*. 2016;1436:118-132.
12. Hekmat D, Mornhinweg R, Bloch G, et al. Macroscopic investigation of the transient hydrodynamic memory behavior of preparative packed chromatography beds. *J Chromatogr A*. 2011;1218:944-950.
13. Khirevich S, Höltzel A, Seidel-Morgenstern A, Tallarek U. Geometrical and topological measures for hydrodynamic dispersion in confined sphere packings at low column-to-particle diameter ratios. *J Chromatogr A*. 2012;1262:77-91.
14. Gritti F, Guiochon G. The current revolution in column technology: how it began, where is it going? *J Chromatogr A*. 2012;1228:2-19.
15. Schmidt-Traub H, Schulte M, Seidel-Morgenstern A. *Preparative Chromatography*. Weinheim, Germany: Wiley-VCH Verlag & Co. KGaA; 2012.
16. Kong DY, Gerontas S, McCluckie RA, Mewies M, Gruberb D, Titchener-Hooker NJ. Effects of bed compression on protein separation on gel filtration chromatography at bench and pilot scale. *Journal of Chemical Technology & Biotechnology*. 2017;93(7):1959-1965.
17. Knox JH, Parcher JF. Effect of column to particle diameter ratio on the dispersion of Unsorbed solutes in chromatography. *Anal Chem*. 1969;41(12):1599-1606.
18. Bruns S, Franklin EG, Grinias JP, Godinho JM, Jorgenson JW, Tallarek U. Slurry concentration effects on the bed morphology and separation efficiency of capillaries packed with sub-2 μm particles. *J Chromatogr A*. 2013;1318:189-197.
19. Kirkland J, DeStefano J. The art and science of forming packed analytical high-performance liquid chromatography columns. *J Chromatogr A*. 2006;1126(1–2):50-57.
20. Martinez A, Kuhn M, Briesen H, Hekmat D. Enhancing the X-ray contrast of polymeric biochromatography particles for three-dimensional imaging. *J Chromatogr A*. 2019;1590:65-72.
21. Reising AE, Godinho JM, Jorgenson JW, Tallarek U. Bed morphological features associated with an optimal slurry concentration for reproducible preparation of efficient capillary ultrahigh pressure liquid chromatography columns. *J Chromatogr A*. 2017;1504:71-82.
22. Reising AE, Schlabach S, Baranau V, Stoeckel D, Tallarek U. Analysis of packing microstructure and wall effects in a narrow-bore ultrahigh pressure liquid chromatography column using focused ion-beam scanning electron microscopy. *J Chromatogr A*. 2017;1513:172-182.
23. Dorn M, Hekmat D. Simulation of the dynamic packing behavior of preparative chromatography columns via discrete particle modeling. *Biotechnol Prog*. 2016;32(2):363-371.
24. Jaeger HM, Nagel SR, Behringer RP. Granular solids, liquids, and gases. *Review of Modern Physics*. 1996;68(4):1259-1273.
25. Hanotin C, Kiesgen de Richter S, Marchal P, Michot LJ, Baravian C. Vibration-induced liquefaction of granular suspensions. *Phys Rev Lett*. 2012;108(19):198301.
26. Lozano C, Luma G, Zuriguel I, Hidalgo RC, Garcimartín A. Breaking arches with vibrations: the role of defects. *Phys Rev Lett*. 2012;109(6):068001.
27. Cao YX, Chakrabortty B, Barker GC, Mehta A, Wang YJ. Bridges in three-dimensional granular packings: experiments and simulations. *Europhysics Letters*. 2013;102(2):24004.
28. Zorica J, Darko V. Compaction dynamics of vibrated granular materials. *Scientific Technical Review*. 2012;62(3):39-44.
29. Chen K, Cole J, Conger C, et al. Packing grains by thermal cycling. *Nature*. 2006;442(7100):257-257.
30. Jia X, Brunet T, Laurent J. Elastic weakening of a dense granular pack by acoustic fluidization: slipping, compaction, and aging. *Physical Review E*. 2011;84(2):020301.
31. Jia X, Caroli C, Velicky B. Ultrasound propagation in externally stressed granular media. *Phys Rev Lett*. 1999;82(9):1863-1866.
32. Tariot A, Gauthier G, Gondret P, et al. Granular compaction by fluidization. *EPJ Web of Conferences*. 2017;140:100003.
33. Reichhardt CJO, Lopatina LM, Jia X, Johnson P. Softening of granular packings with dynamic forcing. *Physical Review E*. 2015;92(2):022203.
34. Dorn M, Eschbach F, Hekmat D, Weuster-Botz D. Influence of different packing methods on the hydrodynamic stability of chromatography columns. *J Chromatogr A*. 2017;1516:89-101.
35. Feeney A, Sikaneta S, Harkness P, Lucas M. An ultrasonic compactor for oil and gas exploration. *Physics Procedia*. 2016;87:72-78.
36. Levina M, Rubinstein MH. The effect of ultrasonic vibration on the compaction characteristics of ibuprofen. *Drug Dev Ind Pharm*. 2002;28(5):495-514.
37. Levina M, Rubinstein MH. The effect of ultrasonic vibration on the compaction characteristics of paracetamol. *J Pharm Sci*. 2000;89(6):705-723.
38. Abedini R, Abdullah A, Alizadeh Y. Ultrasonic assisted hot metal powder compaction. *Ultrason Sonochem*. 2016;38:704-710.
39. Fartashvand V, Abdullah A, Sadough Vanini SA. Effects of high power ultrasonic vibration on the cold compaction of titanium. *Ultrasonic Sonochemistry*. 2017;36:155-161.
40. Franc M, Vojta J, Sobotnikova J, Pavel C, Zuzana B. Performance and lifetime of slurry packed capillary columns for high performance liquid chromatography. *Chemical Papers*. 2013;68(1):22-28.

41. Ehlert S, Rösler T, Tallarek U. Packing density of slurry-packed capillaries at low aspect ratios. *J Sep Sci*. 2008;31(10):1719-1728.
42. Shalliker RA, Broyles BS, Guiochon G. Evaluation of the secondary consolidation of columns for liquid chromatography by ultrasonic irradiation. *J Chromatogr A*. 2000;878(2):153-163.
43. Ehlert S, Kraiczek K, Mora J-A, Dittmann M, Rozing GP, Tallarek U. Separation efficiency of particle-packed HPLC microchips. *Anal Chem*. 2008;80(15):5845-5950.
44. V. Natarajan, A. F. Mann and D. Schubnel, Method of and device for packing a chromatography column. United States of America Patent US20100084342 A1, 8th April 2010.
45. C. V. Company, "www.clevelandvibrator.com," Cleveland Vibrator, 2016. https://www.clevelandvibrator.com/images/Documents/Selection%20Guide%20for%20Industrial%20Vibrators.pdf. [Accessed July 19, 2019].
46. T. Biosciences, "Toyopearl Instruction Manual," Tosoh Biosciences, https://www.separations.eu.tosohbioscience.com/OpenPDF.aspx?path=/File%20Library/TBG/Products%20Download/Instruction%20Manual/m15p73a.pdf. [Accessed January 2019].
47. B. Laboratories, "CHT Ceramic Hydroxyapatite Instruction Manual," BioRad Laboratories, https://www.bio-rad.com/webroot/web/pdf/lsr/literature/LIT611E.PDF. [Accessed January 2019].
48. Deutsch V, Platte M, Vogt M. *Ultraschallprüfung: Grundlagen und industrielle Anwendungen*. Berlin: Springer; 1997.
49. Callens D, Bruneel C, Assaad J. Matching ultrasonic transducer using two matching layers where one of them is glue. *NDT & E Int*. 2004;37(8):591-596.
50. Manh T, Nguyen A-TT, Johansen TF, Hoff L. Microfabrication of stacks of acoustic matching layers for 15 MHz ultrasonic transducers. *Ultrasonics*. 2014;54(2):614-620.
51. Hekmat D, Kuhn M, Meinhardt V, Weuster-Botz D. Modeling of transient flow through a viscoelastic preparative chromatography packing. *Biotechnol Prog*. 2013;29(4):958-967.
52. DePhillips P, Lenhoff AM. Pore size distributions of cation-exchange adsorbents determined by inverse size-exclusion chromatography. *J Chromatogr A*. 2000;883:39-54.
53. Aldak GmbH, "Pneumatic vibrators and knockers," Aldak, 2017. https://www.aldak.com/pneumatic-vibrators/overview.html. [Accessed 29 26 2019].
54. Lei J, Hill M, Glynne-Jones P. Numerical simulation of 3D boundary-driven acoustic streaming in microfluidic devices. *Lab Chip*. 2014;14(3):532-541.
55. Wiklund M, Green R, Ohlin M. Acoustofluidics 14: applications of acoustic streaming in microfluidic devices. *Lab Chip*. 2012;12:2438-2451.
56. Bruus H. Acoustofluidics 7: the acoustic radiation force on. *Lab Chip*. 2012;12:1014-1021.
57. Hawkes JJ, Radel S. Acoustofluidics 22: multi-wavelength resonators, applications and considerations. *Lab Chip*. 2013;13(4):610-627.
58. Carlevaro C, Pugnaloni L. Arches and contact forces in a granular pile. *Eur Phys J E*. 2012;35(6):44.
59. Mehta A. Spatial, dynamical and spatiotemporal heterogeneities in granular media. *Soft Matter*. 2010;6(13):2875-2883.
60. Sternberg JC. Extracolumn contributions to chromatographic band broadening. *Adv Chromatogr*. 1966;2:205-270.

How to cite this article: Martinez A, Knaub K, Monter M, Hekmat D, Weuster-Botz D. Improved packing of preparative biochromatography columns by mechanical vibration. *Biotechnol Progress*. 2020;36:e2950. https://doi.org/10.1002/btpr.2950